



Eidgenössische Technische Hochschule Zürich
Swiss Federal Institute of Technology Zurich



Deep Domain Adaptation by Geodesic Distance Minimization

Semester's Thesis

Yifei Wang

Department of Information Technology and Electrical Engineering

Advisor: Wen Li, and Dengxin Dai
Supervisor: Prof. Dr. Luc Van Gool

April 14, 2017

Abstract

Visual domain adaptation aims to improve the performance of visual recognition models leaned from a source domain to a target domain with a similar but different distribution. Usually, the source domain contains a large number of labeled data for training the models, but the target domain contains only unlabeled data. Visual domain adaptation has attracted more and more attentions from computer vision researchers in recent years. It becomes even more important after the revival of deep learning, because deep learning usually requires a large number of labeled training data to learn a robust model, and it is generally difficult to annotate a large number of training data which follows the identical distribution as the test data.

Recently, a method called deep CORAL was proposed for deep domain adaptation problem. It represents each domain by its second order statistic information (*i.e.* the covariance matrix), and minimizes the Euclidean distance between the covariance matrices of the source domain (training domain) and the target domain (test domain). However, Euclidean distance may not be a proper choice for measuring the difference between covariance matrices, since the covariance matrix is a PSD matrix that represents the second-order statistical information.

In this work, we propose a new method for deep unsupervised domain adaptation. By observing the covariance matrix lies on a Riemannian manifold, we propose to minimize the geodesic distance between the source and target covariance matrices. We build up our method on the deep CORAL approach, and use the Log-Euclidean distance to replace the naive Euclidean distance. In particular, we use the pre-trained Alexnet model as the base model, and add a new LogEig layer after fc8 layer, which calculate Riemannian distance of two covariance matrices from source and target domains. We simultaneously optimize the classification loss on the source domain labeled samples and the Log-Euclidean distance between two domains.

We conduct experiments on the benchmark Office dataset. The results show that Deep LogCORAL gives higher accuracy in four out of the six domains and raise 0.7% of the average accuracy. Also, the experiment gives another interesting observation that Euclidean distance and Riemannian distance have only weak correlation, which shows a potential direction in domain adaptation to optimize Euclidean distance and Riemannian distance at the same time.

Acknowledgements

I would like to express my sincere gratitude to my advisers Wen Liand Dengxin Dai for their guidance and support throughout this project. I also want to thank Dr. Zhiwu Huang for the useful discussion and valuable suggestions on this project.

Contents

1	Introduction	1
1.1	Motivation	1
1.2	Thesis Organization	3
2	Related Work	5
3	Materials and Methods	7
3.1	Hands-on Experiment to Demonstrate Dataset Bias	7
3.2	Review to Deep CORAL Loss	8
3.3	LogEig Layer	10
3.4	Proposed Deep LogCORAL Structure	11
4	Experiments and Results	13
4.1	Reproduce Deep CORAL	13
4.2	Deep LogCORAL	14
5	Discussion	17
6	Conclusion	33

CONTENTS

List of Figures

1.1	Example pictures from Amazon(first row), DSLR(second row) and Webcam(third row)	2
1.2	Illustration of our proposed domain adaptation method: minimizing geodesic distance between two domains in Riemannian manifold.	3
3.1	Structure of Deep CORAL.	9
3.2	Structure of Deep LogCORAL.	11
4.1	Sample learning curve of CNN, Deep CORAL and Deep LogCORAL in domain shift A-W.	15
5.1	Source domain(Amazon) feature extracted after fc8 using CNN.	18
5.2	Target domain(Webcam) feature extracted after fc8 using CNN.	19
5.3	Source domain(Amazon) feature extracted after fc8 using Deep CORAL.	20
5.4	Target domain(Webcam) feature extracted after fc8 using Deep CORAL.	21
5.5	Source domain(Amazon) feature extracted after fc8 using Deep LogCORAL.	22
5.6	Target domain(Webcam) feature extracted after fc8 using Deep LogCORAL.	23
5.7	Source domain covariance matrix using CNN features.	24
5.8	Target domain covariance matrix using CNN features.	25
5.9	Source domain covariance matrix using Deep LogCORAL features.	26
5.10	Target domain covariance matrix using Deep LogCORAL features.	27
5.11	Loss curve of CNN.	28
5.12	Loss curve of Deep CORAL.	29
5.13	Loss curve of Deep LogCORAL.	30
5.14	Number of samples that classified correctly by methods specified in row but fails by methods specified in column.	31

LIST OF FIGURES

List of Tables

3.1	Demonstration of dataset bias on Amazon, Webcam, DSLR, Caltech-256	8
4.1	Accuracy from Deep CORAL.	13
4.2	Accuracy of reproduced results.	13
4.3	Accuracy comparison for the three methods.	14

LIST OF TABLES

Chapter 1

Introduction

1.1 Motivation

Rapid progress recently in computer vision can hardly be achieved without growing of large image databases, since datasets provide crucial evidence to build robust classifiers in image recognition. An ideal dataset for image recognition is one sampled from the identical distribution as the test data, which is also one of the most fundamental assumption in traditional machine learning.

However, in real world visual recognition applications, it is hard to guarantee the existing human-annotated dataset has the identical distribution as the test data in the real world application. Actually, as pointed by Torrabla and Efros [14], each existing visual recognition datasets more or less has its own bias, due to limited ways of acquiring the image and labels when building the dataset. Although it is possible to collect and annotate a new dataset to reduce the distribution difference between training and test data, however, it would be both expensive and time consuming, especially when using deep learning techniques which usually requires a large number of training data.

We take the popular benchmark Office dataset to illustrate the visual domain difference. The Office dataset contains images collected from three domains: *Amazon*, *DSLR*, *Webcam*, each has identically thirty one categories. The Amazon dataset contains object images crowded from amazon website. The Webcam dataset contains images captured by web cameras while the DSLR dataset has images captured by DSLR. Figure 1.1 gives some examples of the same category: bottle. But for different domains they exhibit very different characteristics. Amazon usually has clean background and the viewpoint is always from the front. Webcam and DSLR looks more similar to each other, they contain the same background and variety of viewpoints. However the illustration and the angle of shooting the picture is slightly different. So as one can expect, the model trained on Amazon and tested on DSLR or Webcam would have lower accuracy than model trained on DSLR and tested on Webcam (or the other way round). The experiment on Section 3.1 confirms it.

If we want to train classifier on one domain and apply it to another domain, the performance may drop significantly as the classifier has already memorizing all its idiosyncrasies and losing



Figure 1.1: Example pictures from Amazon(first row), DSLR(second row) and Webcam(third row).

ability to generalize [14]. When training domain and test domain varies too much, having more training data doesn't necessarily guarantee better results. In other words, the classification performance is limited because of domain shift.

Even for nowadays most popular Convolutional Neural Network(CNN) is susceptible to domain shift [3]. After CNN regain its fame after 2012 ImageNet Large Scale Visual Recognition Challenge, almost every highly ranked team in image recognition competition used CNN as their basic framework. If we can overcome the mismatch of domain shift in CNN, we can further improve the generalization capacity of the best classifier we have now.

There have already been many works focusing on domain adaptation. For CNN one of the most effective way is to minimize the second order Euclidean distance between target domain (training domain) and source domain (test domain)[13]. Intuitively, this method shorten the distance between two domain and therefore the model can work better on test domain. The reasoning behind it seems convincing, however before going deeper into this method we need to ask one crucial question: *Is the Euclidean distance a good choice for measuring the distance between the covariance matrices between two domains?*

Intuitively, the covariance matrix is a PSD matrix, which lies on a Riemannian manifold. The source and target covariance matrices can be deemed as two points on the Riemannian manifold, so a more desirable metric is the geodesic distance between the two points on the Riemannian manifold. Actually, minimize Riemannian distance for domain adaptation shows encouraging result in SVM [2]. This motivates us to minimize Riemannian distance based on CNN. Figure 1.2 illus-

tration of our proposed domain adaptation method. \mathbf{C}_s and \mathbf{C}_t represent the covariance matrix of source and target domains respectively. The crosses, triangles and stars in the blue (red) rectangle denote the training samples of different classes from the source (target) domain. We hope to reduce domain shift by minimizing the geodesic distance between these two domains.

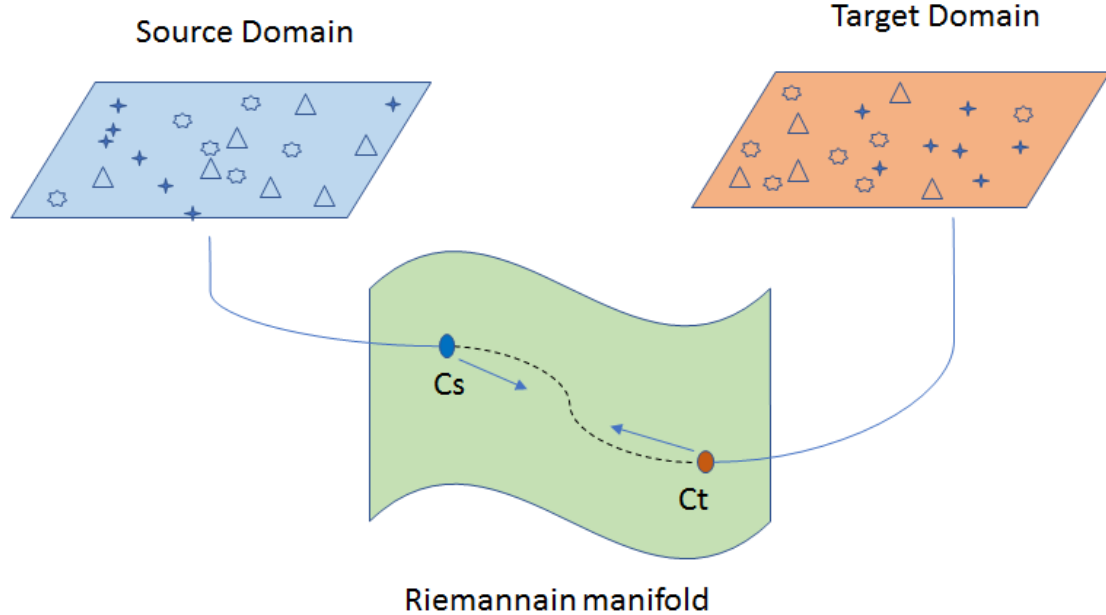


Figure 1.2: Illustration of our proposed domain adaptation method: minimizing geodesic distance between two domains in Riemannian manifold.

1.2 Thesis Organization

To show the process and logic for testifying the assumption. The thesis is organized into six chapters. The first chapter is introduction chapter which gives overview on basic domain adaptation concepts and how we inspired to do this work. The second chapter conveys an overview of the relevant theory and previous work that focus on domain adaptation. For the third part, the logic behind this method and deviation of mathematical formula would be described in detail. Experiment result and its analysis would be introduced in chapter four and five. Possible future work to develop this method is also discussed in chapter five. At last, conclusion is drawn in chapter six.

CHAPTER 1. INTRODUCTION

Chapter 2

Related Work

We briefly review a few works which are closely related to this work. For a comprehension summary for domain adaptation we refer readers to [10]. In [14] the concept of dataset bias was well introduced and draw many people's attention. Since then, many methods have been developed in order to overcome the presenting build-in dataset bias.

Early domain adaptation method like [11] requires to learn a regularized transformation using information-theoretic metric learning that maps data in the source domain to the target domain. However this method require labeled data from target domain which in many scenarios is unknown to testers. Later unsupervised domain adaptation method [6][5][4][12][2] tried to improve the performance on test domain by transferring knowledge from test domain to training domain without the need of test labels. In [6] first extract features that invariant to domain change then model the different domains as points on Grassmann manifold and generate number of subspaces in between to train classifier on those subspaces. In [5] further develop the idea to use multiple kernels to generate subspaces. Similarly, to cut back the difference between training set and test set [2] generate subspaces in Riemannian manifold and [12] measure distance in Euclidean distance. In [4] source and target domains are represented by subspaces described by eigen vectors and then learning a mapping function which aligns the two domains.

More related with this paper is domain adaptation method applying in CNN. In [15], it proposes a new CNN architecture which introduces an adaptation layer and an additional main confusion loss to learn a representation. In [9], it also presents a new architecture where hidden representations of all task-specific layers are embedded in a reproducing kernel Hilbert space where the mean embedding of different domain distributions can be explicitly matched.

Our work is most related and inspired by [13] which adds a new CORAL loss that calculate the Euclidean distance of two domain's covariance matrices before softmax layer. This method looks very simple but the result shows it exceeds other methods which appears to be more complex and it holds highest classification accuracy on Office dataset for unsupervised domain adaptation. Another paper is about symmetric positive definite (SPD) matrix learning [7], where it present a new direction of SPD matrix non-linear learning in deep neural network model.

CHAPTER 2. RELATED WORK

Chapter 3

Materials and Methods

This chapter will introduce the concept and mathematical derivation behind the work.

3.1 Hands-on Experiment to Demonstrate Dataset Bias

Now we get the concept about dataset bias and we know that dataset bias would significantly influence the performance of classifier. In machine learning, we always assume that the data distribution in source domain and target domain is the same, nevertheless it seldom meets the requirement in reality. To demonstrate the existence of dataset bias and how it can affect the test accuracy, we give a simple experiment by using the benchmark Office dataset.

We follow the experimental setting followed in [6], which uses the extracted SURF features provided in [6] on four datasets: Amazon, Webcam, DSLR, Caltech-256 with ten common classes. We use the common machine learning method support vector machine(SVM) and nearest neighbors(NN) to demonstrate the result.

The experiment result shows in Table 3.1. Note that A represents Amazon, D represents DSLR, W represents Webcam, D represents Caltech-256. And we also use the same abbreviation in the remaining chapters. As show in Table 3.1, we observe that a model tested on a different domain may have a significant drop in terms of classification accuracy. For example, the SVM model trained on DSLR has an accuracy of 66.63% when testing on Webcam. However if we use SVM model trained on Amazon, it has a much lower accuracy of 30.38% when testing on the same Webcam domain. In fact, the Amazon domain has more training data than the DSLR domain, the performance is still much worse due to the larger domain distribution mismatch with the test domain Webcam. This clearly demonstrates the significant influence of domain shift to image classification.

Table 3.1: Demonstration of dataset bias on Amazon, Webcam, DSLR, Caltech-256

Source to Target domain	Accuracy (%)	
	SVM	NN
C - A	42.04	31.55
C - W	33.71	28.47
C - D	39.71	30.93
A - C	36.88	27.71
A - W	34.55	27.38
A - D	34.13	28.59
W - C	28.07	24.56
W - A	33.49	31.17
W - D	70.83	59.61
D - C	29.27	26.88
D - A	30.38	30.52
D - W	66.63	57.97

3.2 Review to Deep CORAL Loss

We build our methodology on the deep CORAL method [13], so we firstly give a brief review of deep CORAL method. Figure 3.1 shows the structure proposed in [13]. It uses a correlation alignment layer after the fc8 layer to calculate the second order distance between two domains.

For generalization and computational simplicity Deep CORAL used AlexNet [8] pre-trained model, therefore our work also implement this structure in order to do a fair comparison.

As described in [13], CORAL loss is built between two domains for a single feature layer. Suppose $\mathbf{D}_S = [\mathbf{x}_1, \dots, \mathbf{x}_{n_S}]$, is source domain features that are extracted out of fc7 layer, x_i is the i -th source sample with d dimension of features. $\mathbf{D}_T = [\mathbf{u}_1, \dots, \mathbf{u}_{n_T}]$ is target domain features that are extracted out of fc7 layer in the same way, similarly u_i is the i -th target sample.

According to [13], CORAL loss is defined as squared Euclidean distance between second order statistics, i.e. covariances of two domains:

$$L_{CORAL} = \frac{1}{4d^2} \|\mathbf{C}_S - \mathbf{C}_T\|^2 \quad (3.1)$$

The covariance matrices \mathbf{C}_S and \mathbf{C}_T are given as follows:

$$\mathbf{C}_S = \frac{1}{n_S - 1} (\mathbf{D}_S^T \mathbf{D}_S - \frac{1}{n_S} (\mathbf{1}^T \mathbf{D}_S)^T (\mathbf{1}^T \mathbf{D}_S)) \quad (3.2)$$

$$\mathbf{C}_T = \frac{1}{n_T - 1} (\mathbf{D}_T^T \mathbf{D}_T - \frac{1}{n_T} (\mathbf{1}^T \mathbf{D}_T)^T (\mathbf{1}^T \mathbf{D}_T)) \quad (3.3)$$

where n_S, n_T is the batch size of the source domain and target domain respectively. $\mathbf{1}^T$ is a vector that all elements equals to 1.

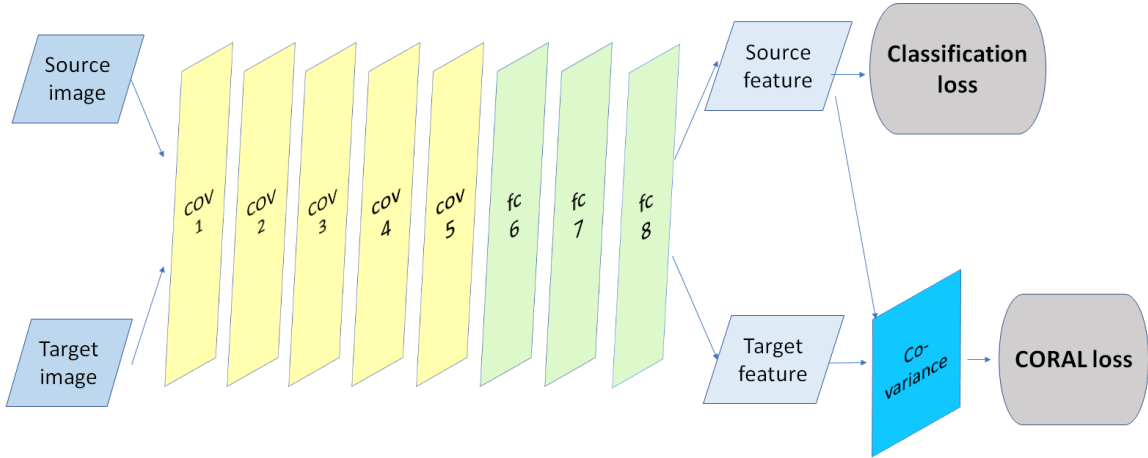


Figure 3.1: Structure of Deep CORAL.

Originally, the correlation alignment layer is one integrated layer that calculate covariance and give out CORAL loss. For convenience of developing our method, we split this integrated layer into two separate layers: covariance layer that calculates covariance matrix and Euclidean loss layer that calculate CORAL loss. Note that the function of these two layers is the same as original correlation alignment layer. So for forward propagation, covariance layer output is Equation (3.2) and (3.3), Equation (3.1) is the forward output of Euclidean loss layer.

For back-propagation. First lets derive for Euclidean loss layer:

$$\frac{\partial L_{CORAL}}{\partial \mathbf{C}_S} = \frac{1}{2d^2}(\mathbf{C}_S - \mathbf{C}_T) \quad (3.4)$$

$$\frac{\partial L_{CORAL}}{\partial \mathbf{C}_T} = -\frac{1}{2d^2}(\mathbf{C}_S - \mathbf{C}_T) \quad (3.5)$$

For back-propagation process in covariance layer, the gradient can be written as:

$$\frac{\partial \mathbf{C}_S}{\partial \mathbf{D}_S} = \frac{2}{n_S - 1}(\mathbf{D}_S - \frac{1}{n_S} \mathbf{1}(\mathbf{1}^T \mathbf{D}_S)^T) \quad (3.6)$$

$$\frac{\partial \mathbf{C}_T}{\partial \mathbf{D}_T} = \frac{2}{n_T - 1}(\mathbf{D}_T - \frac{1}{n_T} \mathbf{1}(\mathbf{1}^T \mathbf{D}_T)^T) \quad (3.7)$$

If CNN only minimizes classification error, it may become overfitting to training set. Add CORAL loss can prevent classifier from adapting too much on source domain and at the same time push classifier to be **closer** to target domain. To push classifier **closer to target domain**, an essential question is to precisely model the distance between two domains. Deep CORAL use squared Euclidean distance to measure distance, while evidence shows that measure distance on other manifolds such as Riemannian manifold may be more precise in measuring matrix distance and can get better result in domain adaptation [7]. To verify this assumption, a new LogEig layer is designed to measure distance in Riemannian manifold.

3.3 LogEig Layer

Covariance matrix is a symmetric semi-positive definite matrix, but adding a small ϵ to the eigenvalues of covariance matrix can transform it into SPD without significantly change its property. Therefore after getting covariance matrix from source and target domain we can apply the method described in [7] to calculate the LogCORAL distance between two covariance matrices.

- *Log-Euclidean Riemannian metric:* Log-Euclidean metrics is first proposed in [1], as stated in the paper it has the capacity to endow Riemannian manifold and also demonstrated that the swelling effect which is clearly visible in the Euclidean case disappears in Riemannian cases. Logarithm operation on the eigenvalue of SPD matrices make the manifold to be flat and then Euclidean distance can be calculate on this flat space. According to [1], this Log-Euclidean computation is easier than other Riemannian computations.
- *LogEig Layer Forward Propagation:* forward is easy to be done by doing singular value decomposition(SVD) to get the eigenvalues and eigenvectors of the covariance metric and get logarithm operation on it:

$$\mathbf{X}_k = \log(\mathbf{X}_{k-1}) = \mathbf{U}_{k-1} \log(\Sigma_{k-1}) \mathbf{U}_{k-1}^T \quad (3.8)$$

where Σ is obtained from SVD for: $\mathbf{X}_{k-1} = \mathbf{U}_{k-1} \Sigma_{k-1} \mathbf{V}_{k-1}^T$, since \mathbf{X} is from covariance matrix so $\mathbf{U} = \mathbf{V}$, thus we can get $\mathbf{X}_{k-1} = \mathbf{U}_{k-1} \Sigma_{k-1} \mathbf{U}_{k-1}^T$. Also k denote the k -th layer. \mathbf{X}_k is the output blob data of the k -th layer. $\log()$ operation is the operation that does logarithm calculation on the diagonal element of the matrix.

- *LogEig Layer Back Propagation:* Back-propagation can be derived using a similar technique as described in [7]:

$$\frac{\partial L}{\partial \mathbf{X}_{k-1}} = \frac{\partial \mathbf{L}}{\partial \mathbf{X}_k} \frac{\partial \log(\mathbf{X}_{k-1})}{\partial \mathbf{X}_{k-1}} \quad (3.9)$$

Where \mathbf{L} is the LogCORAL loss.

$$\frac{\partial L}{\partial \mathbf{X}_{k-1}} = \mathbf{U} (\mathbf{P}^T \circ (\mathbf{U}^T d\mathbf{U}))_{sym} \mathbf{U}^T + \mathbf{U} (d\Sigma)_{diag} \mathbf{U}^T \quad (3.10)$$

where:

$$d\mathbf{U} = 2 \left(\frac{\partial \mathbf{L}_{k+1}}{\partial \mathbf{X}_k} \right)_{sym} \mathbf{U} \log(\Sigma) \quad (3.11)$$

$$d\Sigma = \Sigma^{-1} \mathbf{U}^T \left(\frac{\partial \mathbf{L}_{k+1}}{\partial \mathbf{X}_k} \right)_{sym} \mathbf{U} \quad (3.12)$$

$$\mathbf{P}(i, j) = \begin{cases} \frac{1}{\sigma_i - \sigma_j}, & i \neq j, \\ 0, & i = j \end{cases} \quad (3.13)$$

where \circ is Hadamard product, i.e. element wise product, sym operation is: $\mathbf{A}_{sym} = \frac{1}{2}(\mathbf{A} + \mathbf{A}^T)$, $diag$ operation is \mathbf{A}_{diag} , i.e. \mathbf{A} only keep diagonal value and the rest set to zeros. σ_i denotes the i -th eigenvalue in Σ .

3.4 Proposed Deep LogCORAL Structure

After implementing the LogEig layer, we can build our Deep LogCORAL structure. Same as in Deep CORAL, we have source domain with label and target domain without label. Based on the structure of Deep CORAL we add our LogEig layer between covariance layer and Euclidean loss layer, see figure 3.2.

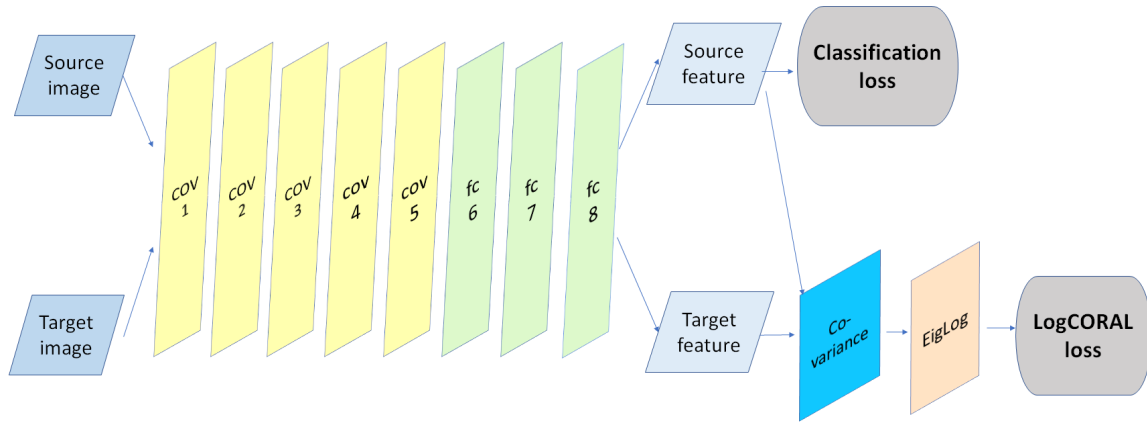


Figure 3.2: Structure of Deep LogCORAL..

CHAPTER 3. MATERIALS AND METHODS

Chapter 4

Experiments and Results

This chapter describes how we carry out the experiment in details. We use Caffe as our deep learning platform and MatCaffe as interface for analysis.

For fair comparison, we follow the experimental setting in Deep CORAL, *i.e.*, using the Office dataset which includes Amazon, Webcam, DSLR and applying AlexNet as pretrained model to perform finetuning.

4.1 Reproduce Deep CORAL

As stated in section 3.2, we first split the original integrated CORAL loss layer into two layers for the simplicity of building our Deep LogCoral structure. The structure is showed in Figure 4.1.

According to [13] the result is showed in table 4.1.

Table 4.1: Accuracy from Deep CORAL.

Accuracy	A - W	D - W	A - D	W - D	W - A	D - A	AVG
CNN	61.6 ± 0.5	95.4 ± 0.3	63.8 ± 0.5	99.0 ± 0.2	49.8 ± 0.4	51.1 ± 0.6	70.10
D-CORAL	66.4 ± 0.4	95.7 ± 0.3	66.8 ± 0.6	99.2 ± 0.1	51.5 ± 0.3	52.8 ± 0.2	72.1

The reproduced result is presented in Table 4.2.

Table 4.2: Accuracy of reproduced results.

Accuracy	A - W	D - W	A - D	W - D	W - A	D - A	AVG
CNN	63.3 ± 0.9	95.2 ± 0.5	65.2 ± 1.3	99.3 ± 0.1	49.2 ± 0.2	51.3 ± 0.4	70.6
D-CORAL	66.1 ± 0.4	95.2 ± 0.5	66.4 ± 2.5	99.2 ± 0.1	50.7 ± 0.2	53.1 ± 0.7	71.8

From these two tables, we can observe that the accuracy deviation is within tolerance. After

optimizing the CORAL loss, average accuracy is improved by 1.2% when comparing with CNN. By using the CORAL loss, the classifier performance can be improved to some extent. Next we will investigate if optimizing LogCORAL loss would get even better results.

4.2 Deep LogCORAL

Our deep LogCORAL is built up on Deep CORAL. Instead of optimizing the Euclidean distance, Deep LogCORAL optimize Riemannian distance. The experiment is carried out according to the structure of Figure 3.1, our newly proposed Deep LogCORAL employs a LogEig layer proposed in Section 3.3 between covariance layer and Euclidean loss layer. A visualization of Caffe structure is shown in Figure 3.2.

Experiment result shows in Table 4.3 along with the result of CNN and Deep CORAL.

Table 4.3: Accuracy comparison for the three methods.

Accuracy	A - W	D - W	A - D	W - D	W - A	D - A	AVG
CNN	63.3 \pm 0.9	95.2 \pm 0.5	65.2 \pm 1.3	99.3 \pm 0.1	49.2 \pm 0.2	51.3 \pm 0.4	70.6
D-CORAL	66.1 \pm 0.4	95.2\pm0.5	66.4 \pm 2.5	99.2 \pm 0.1	50.7 \pm 0.2	53.1\pm0.7	71.8
D-LogCORAL	68.8\pm0.6	95.2 \pm 0.2	68.6\pm1.4	99.5\pm0.4	50.9\pm0.3	51.7 \pm 0.6	72.5

After applying Deep LogCORAL, the average accuracy of the six domain adaptation raised 1.9% and 0.7% compared to CNN and Deep CORAL. In four out of six shifts, it achieves the highest accuracies among all three methods. For the other two shift, the gap between our method and the best result get so far is also small. Note that due to limited time of this project, other than domain shift A-W the other five domain shifts are not well adjusted to find the best weight coefficient for the LogCORAL loss. We believe that the performance would be better under finer adjustment in the future.

We use Amazon as the source domain and Webcam as the target domain to show how Deep LogCORAL works. In Figure 4.3, we show one example of learning curve for CNN, Deep CORAL, Deep LogCORAL. From the figure, we clearly observe that CORAL loss helps to get better result than CNN and optimizing LogCORAL loss helps to achieve much better performance than the two.

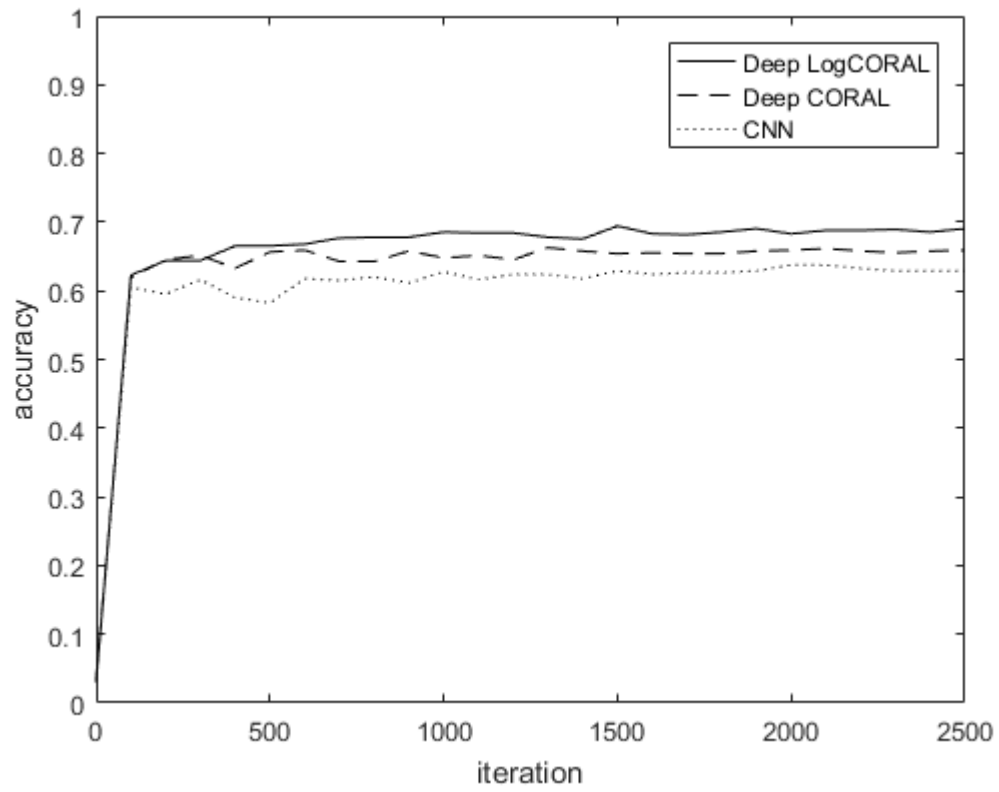


Figure 4.1: Sample learning curve of CNN, Deep CORAL and Deep LogCORAL in domain shift A-W.

CHAPTER 4. EXPERIMENTS AND RESULTS

Chapter 5

Discussion

In this section, we take A-W as an example to better understand how Deep LogCORAL works.

- *What the extracted feature looks like before and after domain adaptation?*

We first train our model on Amazon, and use Webcam to test the model. Then visualize the extracted source and target domain features to gain insight into the model. In Figure 5.1-5.6, we use the t-SNE algorithm to transfer the high dimensional features into two-dimensional feature, and plot points using different colors according to their categories. Intuitively, we expect that if the features can be easier to be linearly separable, the model's generalization capacity would be better. It can be observed that the features are extracted by Deep LogCORAL is easier to be linearly separable according to Figure 5.6.

- *How the covariance matrix look like?*

To visualize how Deep LogCORAL model minimizes the distance between two domains, we plot the covariance matrices of two domains after feeding source and target domain image in CNN and Deep LogCORAL respectively. See Figure 5.7-5.10. Clearly distance is shorter after optimize LogCORAL loss.

- *How Euclidean distance and Riemannian distance correlated?*

After comparing two methods that optimize Euclidean distance and Riemannian distance, we further investigate how those two distances related to each other. Are they correlated to each other considering both try to minimize the difference between two covariance matrices under certain distance metric?

In order to compare the two distance measurements. We plot three loss curves using CNN, Deep CORAL and Deep LogCORAL respectively, see Figure 5.11-5.13, to have an overview of how CORAL loss and LogCORAL loss change when use different methods and whether those two ways of measuring distance correlated or contradictory to each other.

From Figure 5.9 we observe that, without optimizing any of those distances, CORAL loss and LogCORAL loss would both go up. When optimizing CORAL loss, LogCORAL loss

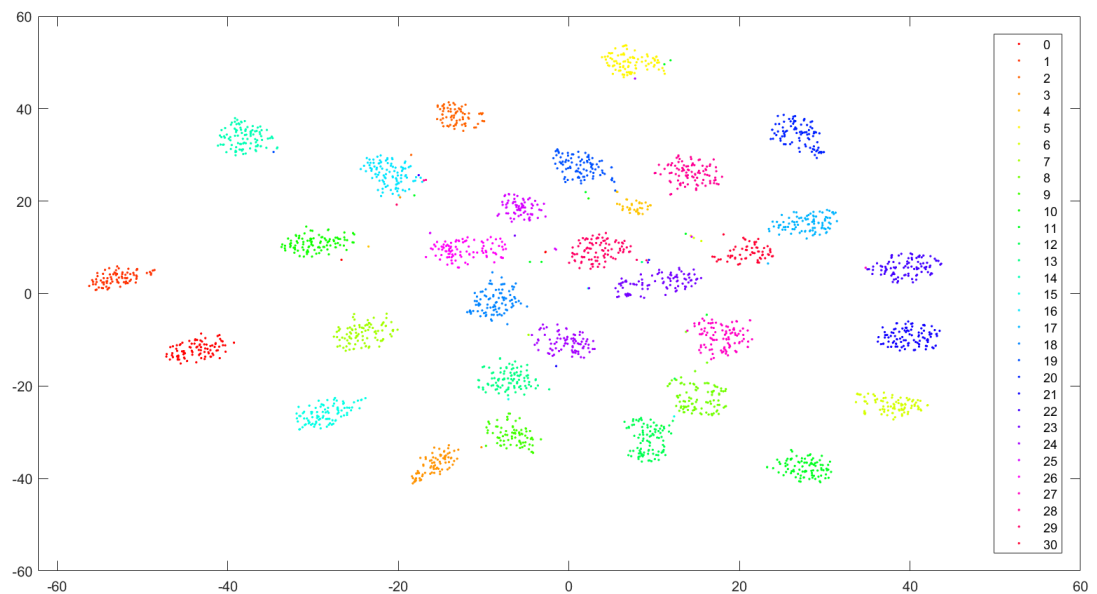


Figure 5.1: Source domain(Amazon) feature extracted after fc8 using CNN.

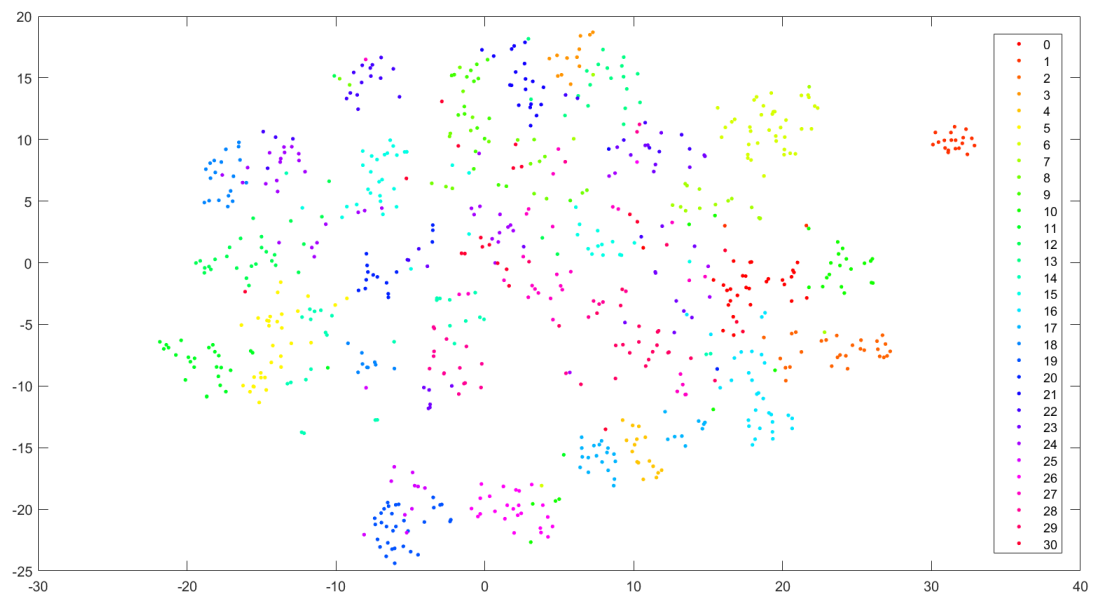


Figure 5.2: Target domain(Webcam) feature extracted after fc8 using CNN.

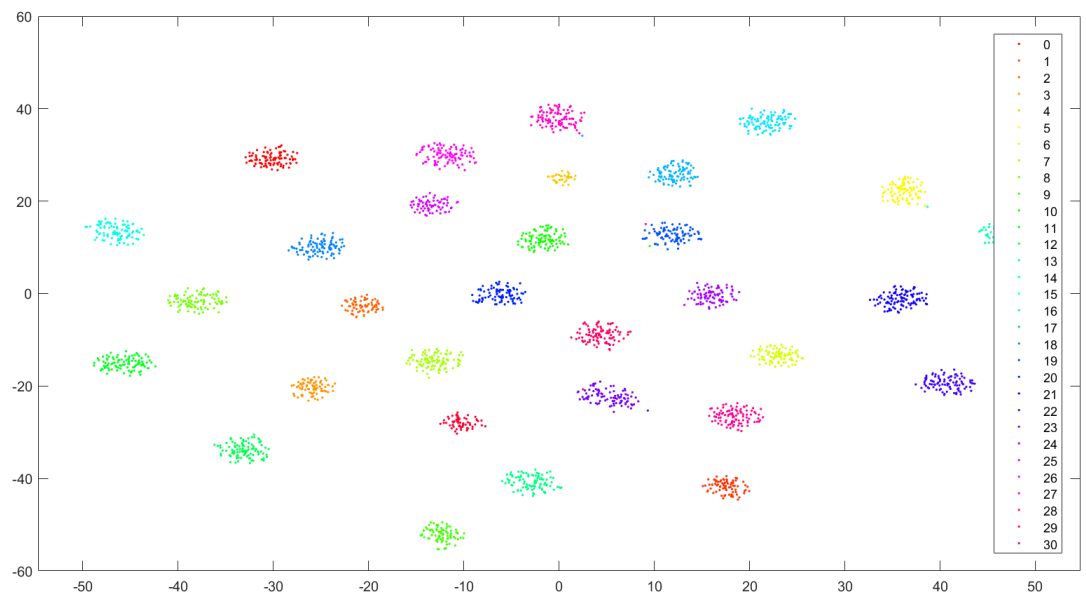


Figure 5.3: Source domain(Amazon) feature extracted after fc8 using Deep CORAL.

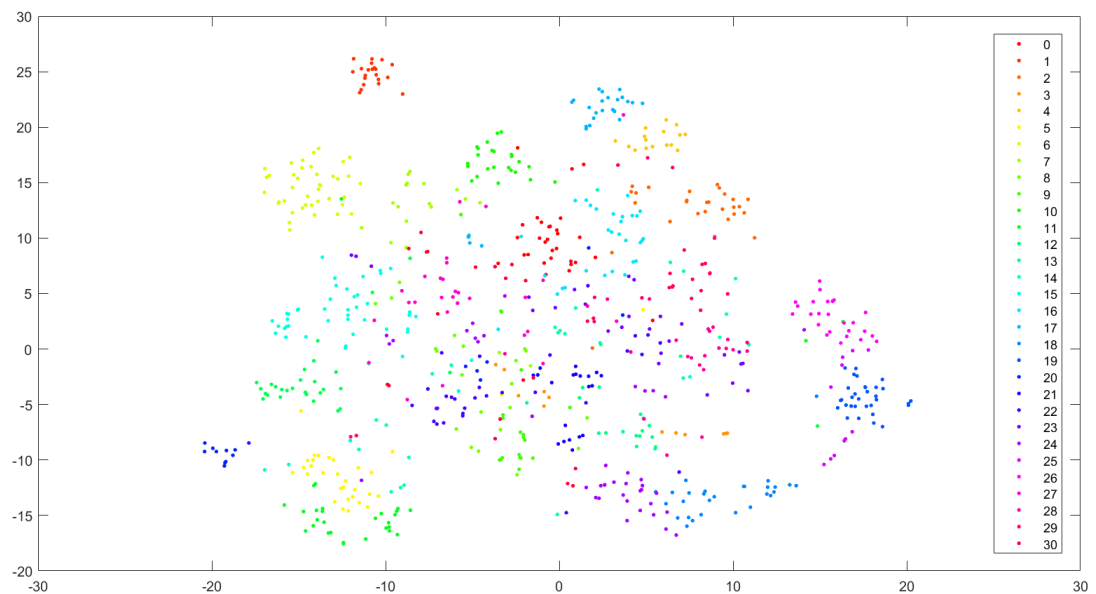


Figure 5.4: Target domain(Webcam) feature extracted after fc8 using Deep CORAL.

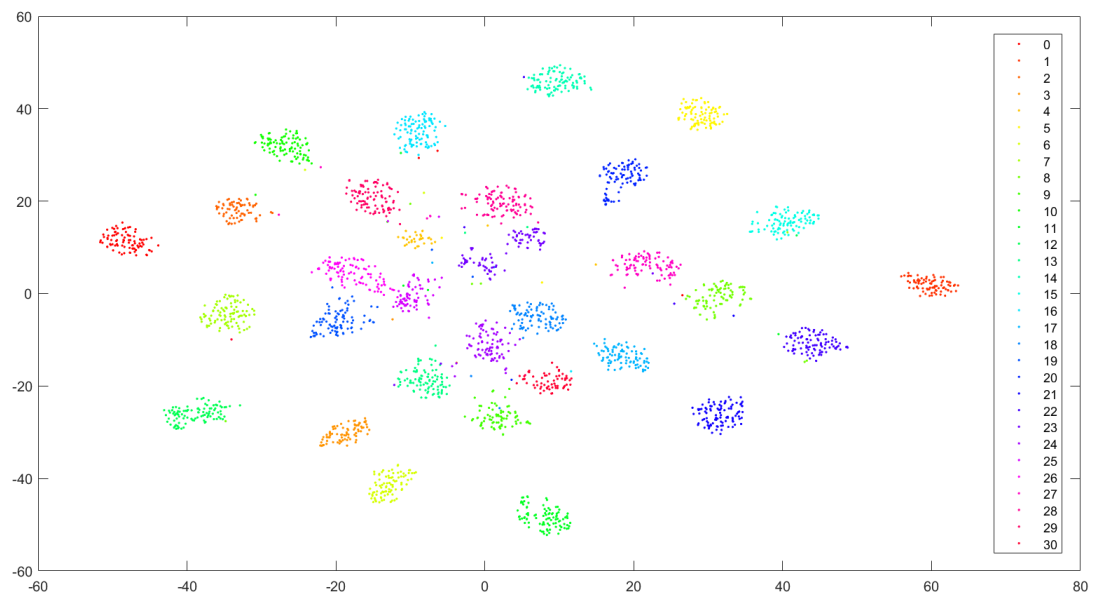


Figure 5.5: Source domain(Amazon) feature extracted after fc8 using Deep LogCORAL.

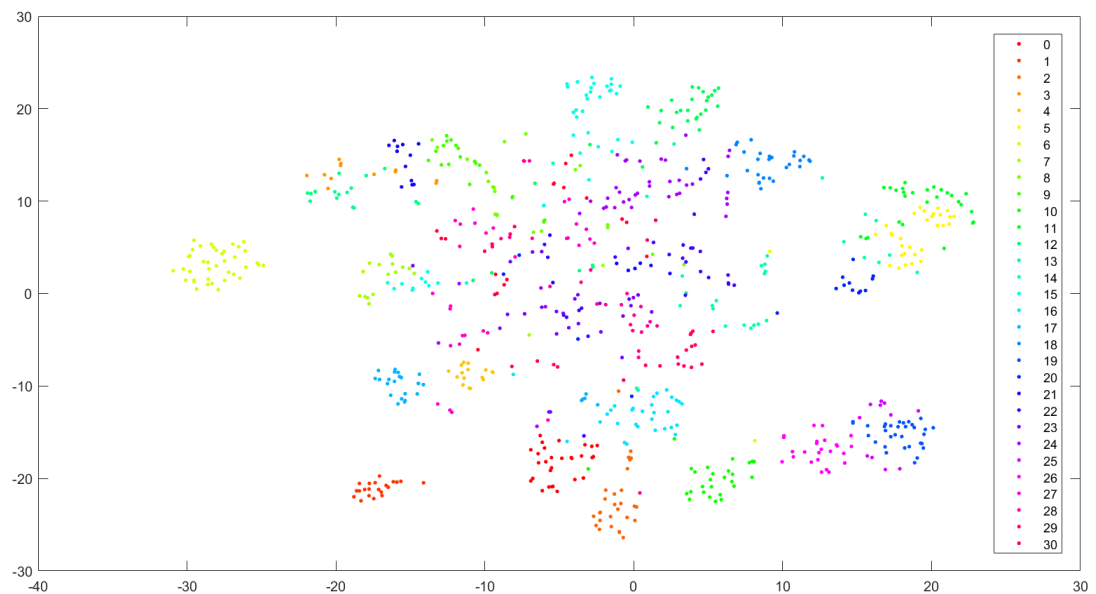


Figure 5.6: Target domain(Webcam) feature extracted after fc8 using Deep LogCORAL.

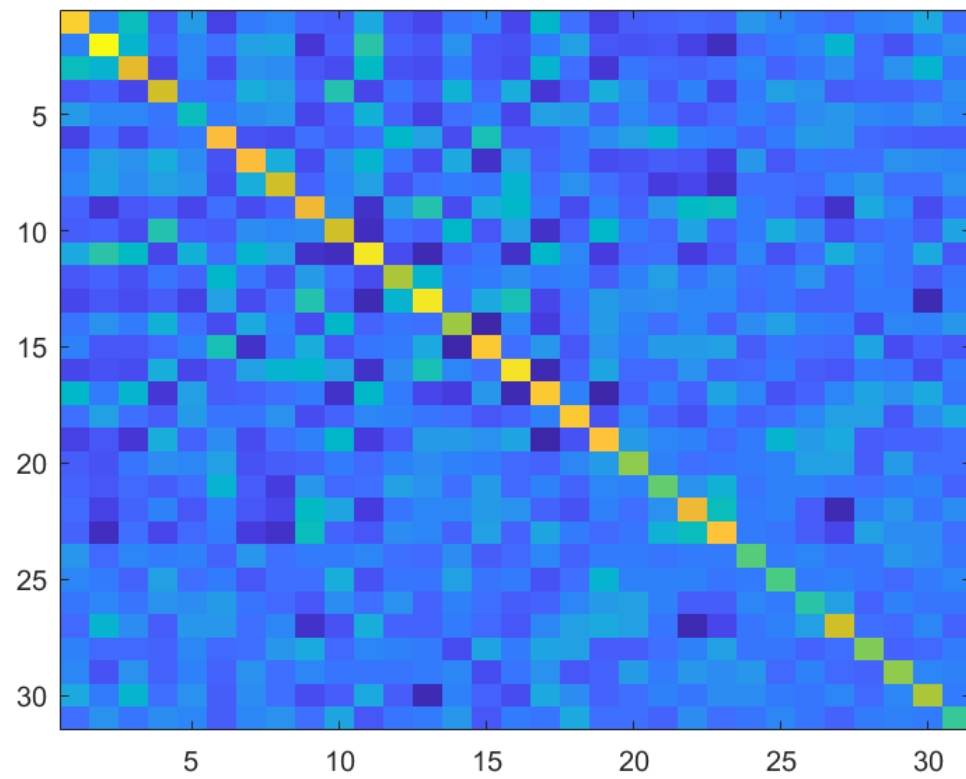


Figure 5.7: Source domain covariance matrix using CNN features.

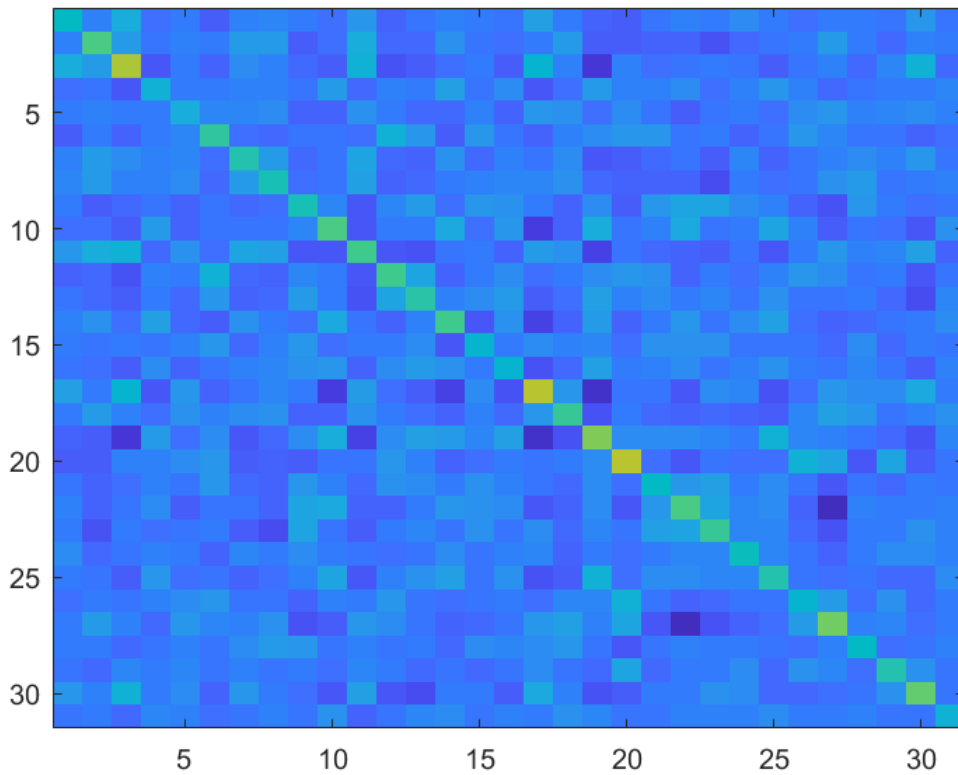


Figure 5.8: Target domain covariance matrix using CNN features.

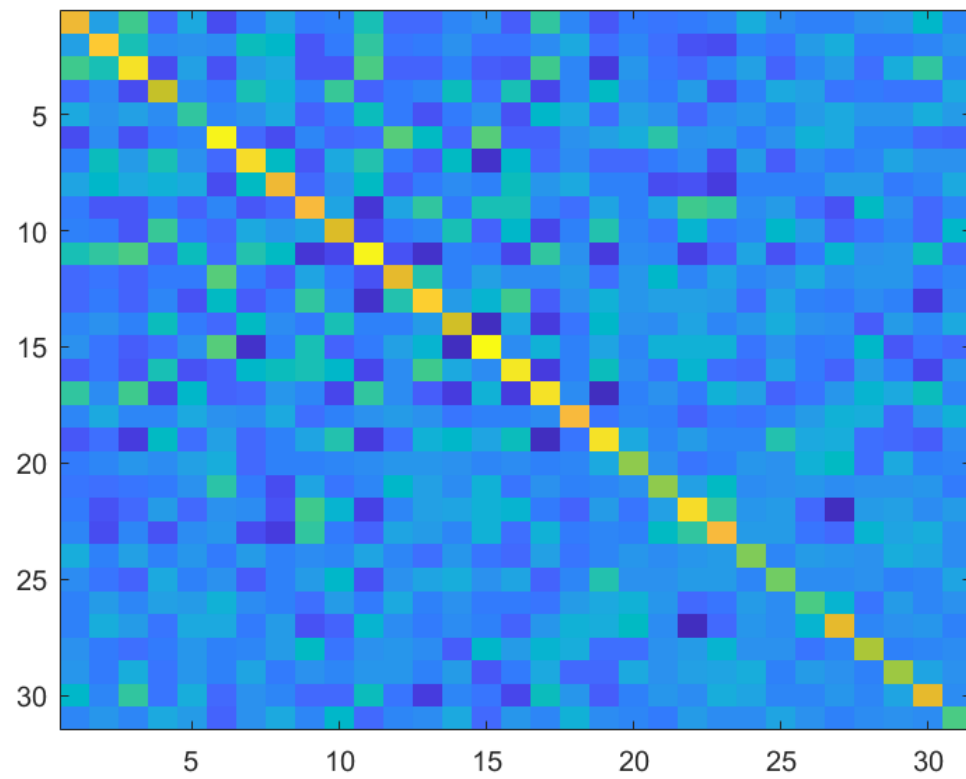


Figure 5.9: Source domain covariance matrix using Deep LogCORAL features.

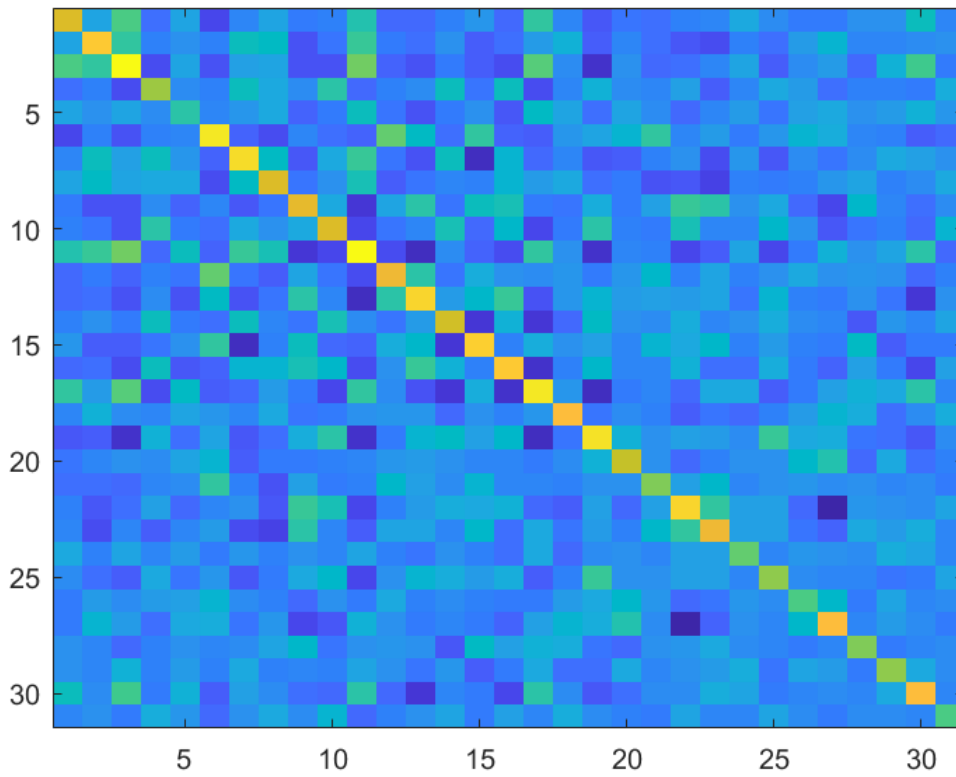


Figure 5.10: Target domain covariance matrix using Deep LogCORAL features.

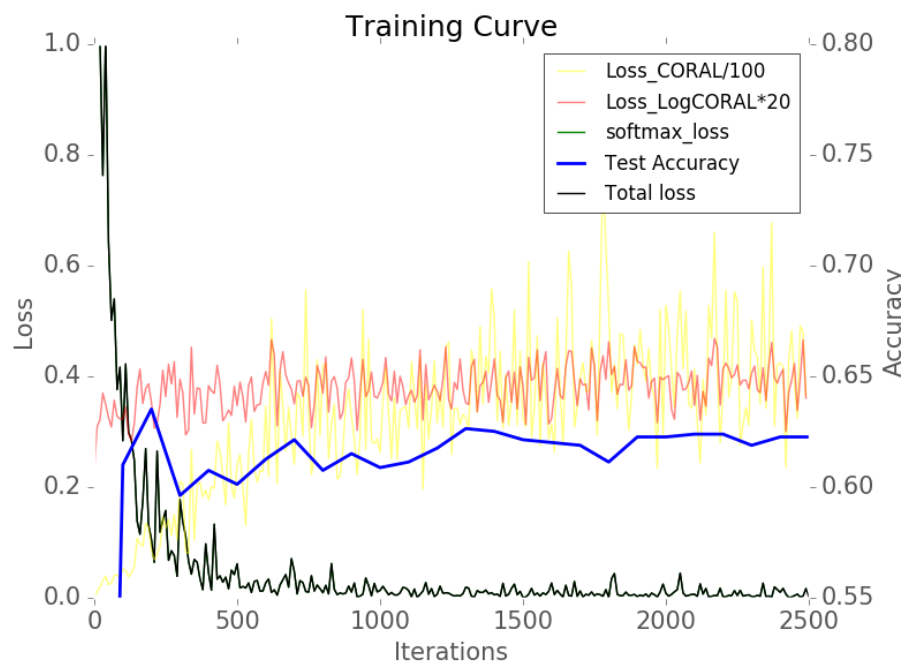


Figure 5.11: Loss curve of CNN.

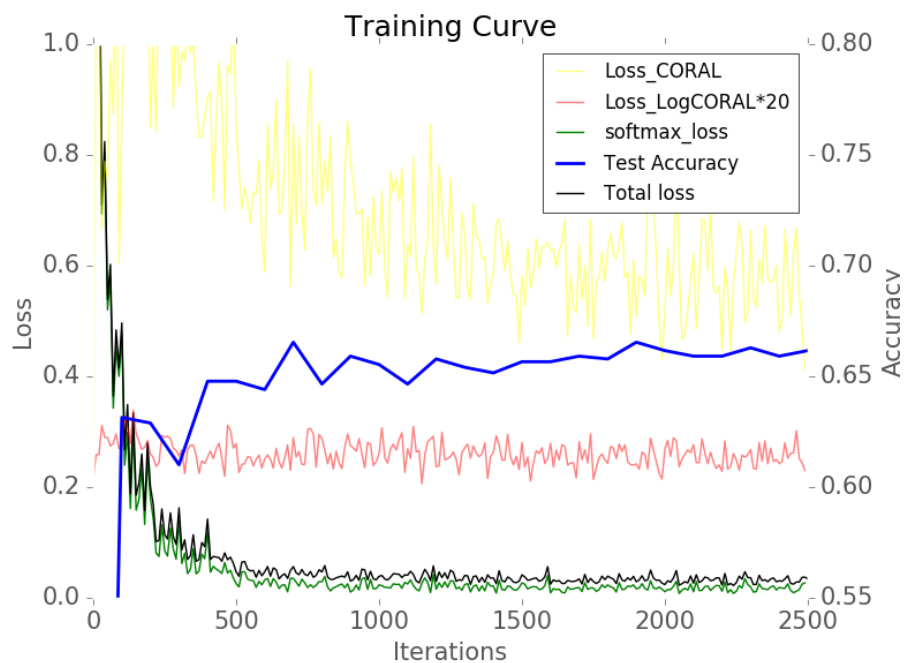


Figure 5.12: Loss curve of Deep CORAL.

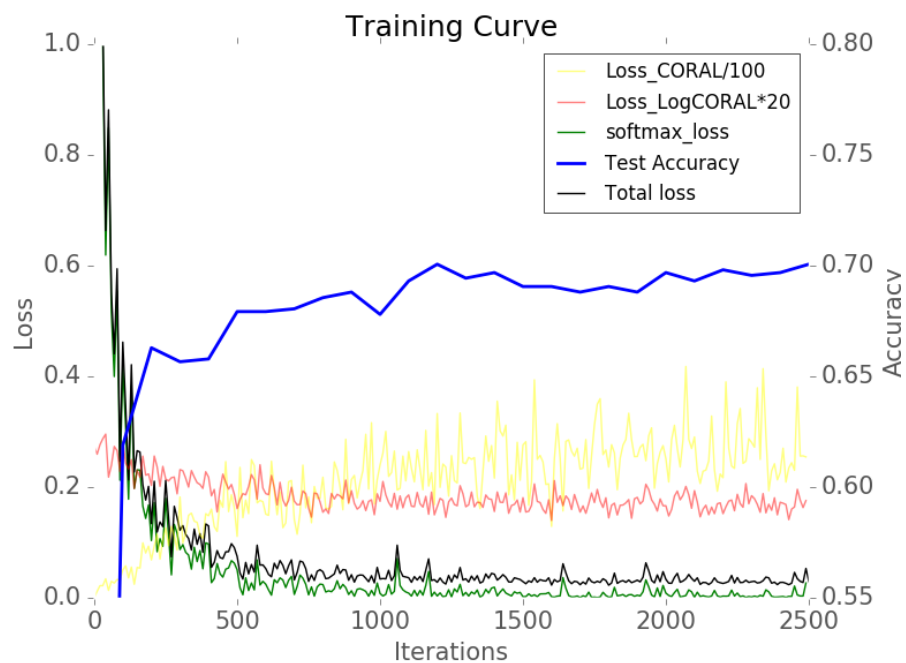


Figure 5.13: Loss curve of Deep LogCORAL.

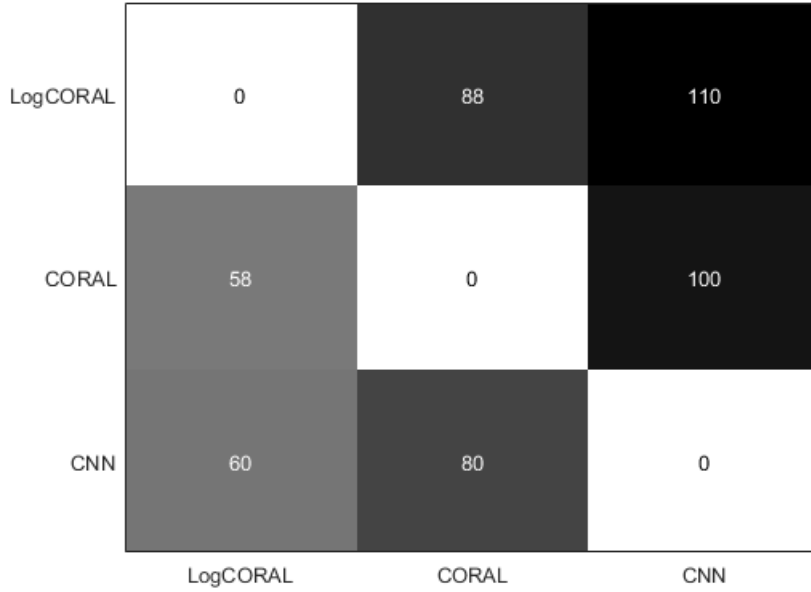


Figure 5.14: Number of samples that classified correctly by methods specified in row but fails by methods specified in column.

remain stable while CORAL loss has a obvious drop down, see Figure 5.10. However if we optimize LogCORAL loss in Figure 5.11, LogCORAL loss goes down but CORAL loss still goes up. So judging from the loss change, it looks like that those two losses have very weak correlation. Since optimize one of these distances alone can raise the classification accuracy to some extent while these distances are not related, combining the distances *i.e.* optimizing the two distances at the same time may achieve even better accuracy.

From Figure 4.3 it's clear that Deep LogCORAL has higher classification accuracy, but how do Deep LogCORAL improve the accuracy? How many samples that can be uniquely classified correctly by LogCORAL or the other methods? Figure 5.14 shows the comparison of how many sample numbers that classified right by one method but fails by the other. Note that Webcam contains 795 images.

From Figure 5.14, its easy to see that LogCORAL can uniquely classify correctly more samples than CNN and CORAL and it is also evidence that Deep LogCORAL has better generalization ability.

CHAPTER 5. DISCUSSION

Chapter 6

Conclusion

In this project, based on the structure of Deep CORAL which minimizes the Euclidean loss, we proposed a new Deep LogCORAL method to minimize the geodesic distance on Riemannian manifold. We used the Log-Euclidean distance to replace the Euclidean distance in the Deep CORAL method. Our experimental results improved performance in unsupervised domain adaptation using the benchmark Office dataset. Besides, experiment indicate that Euclidean distance and Riemannian distance have only weak correlation, therefore this project also shows potential direction for the future domain adaptation work to optimize Euclidean distance and Riemannian distance at the same time.

CHAPTER 6. CONCLUSION

Bibliography

- [1] Vincent Arsigny, Pierre Fillard, Xavier Pennec, and Nicholas Ayache. Geometric means in a novel vector space structure on symmetric positive-definite matrices. *SIAM journal on matrix analysis and applications*, 29(1):328–347, 2007.
- [2] Zhen Cui, Wen Li, Dong Xu, Shiguang Shan, Xilin Chen, and Xuelong Li. Flowing on riemannian manifold: Domain adaptation by shifting covariance. *IEEE transactions on cybernetics*, 44(12):2264–2273, 2014.
- [3] Jeff Donahue, Yangqing Jia, Oriol Vinyals, Judy Hoffman, Ning Zhang, Eric Tzeng, and Trevor Darrell. Decaf: A deep convolutional activation feature for generic visual recognition. In *Icml*, volume 32, pages 647–655, 2014.
- [4] Basura Fernando, Amaury Habrard, Marc Sebban, and Tinne Tuytelaars. Unsupervised visual domain adaptation using subspace alignment. In *Proceedings of the IEEE International Conference on Computer Vision*, pages 2960–2967, 2013.
- [5] Boqing Gong, Fei Sha, and Kristen Grauman. Overcoming dataset bias: An unsupervised domain adaptation approach. In *NIPS Workshop on Large Scale Visual Recognition and Retrieval*, volume 3. Citeseer, 2012.
- [6] Boqing Gong, Yuan Shi, Fei Sha, and Kristen Grauman. Geodesic flow kernel for unsupervised domain adaptation. In *Computer Vision and Pattern Recognition (CVPR), 2012 IEEE Conference on*, pages 2066–2073. IEEE, 2012.
- [7] Zhiwu Huang and Luc Van Gool. A riemannian network for spd matrix learning. *arXiv preprint arXiv:1608.04233*, 2016.
- [8] Alex Krizhevsky, Ilya Sutskever, and Geoffrey E Hinton. Imagenet classification with deep convolutional neural networks. In *Advances in neural information processing systems*, pages 1097–1105, 2012.
- [9] Mingsheng Long, Yue Cao, Jianmin Wang, and Michael I Jordan. Learning transferable features with deep adaptation networks. In *ICML*, pages 97–105, 2015.

BIBLIOGRAPHY

- [10] Vishal M Patel, Raghuraman Gopalan, Ruonan Li, and Rama Chellappa. Visual domain adaptation: A survey of recent advances. *IEEE signal processing magazine*, 32(3):53–69, 2015.
- [11] Kate Saenko, Brian Kulis, Mario Fritz, and Trevor Darrell. Adapting visual category models to new domains. *Computer Vision–ECCV 2010*, pages 213–226, 2010.
- [12] Baochen Sun, Jiashi Feng, and Kate Saenko. Return of frustratingly easy domain adaptation. *arXiv preprint arXiv:1511.05547*, 2015.
- [13] Baochen Sun and Kate Saenko. Deep coral: Correlation alignment for deep domain adaptation. In *Computer Vision–ECCV 2016 Workshops*, pages 443–450. Springer, 2016.
- [14] Antonio Torralba and Alexei A Efros. Unbiased look at dataset bias. In *Computer Vision and Pattern Recognition (CVPR), 2011 IEEE Conference on*, pages 1521–1528. IEEE, 2011.
- [15] Eric Tzeng, Judy Hoffman, Ning Zhang, Kate Saenko, and Trevor Darrell. Deep domain confusion: Maximizing for domain invariance. *arXiv preprint arXiv:1412.3474*, 2014.